THE ASTROPHYSICAL JOURNAL, 302:606–610, 1986 March 15

EXOSAT AND *EINSTEIN* X-RAY OBSERVATIONS OF THE SNR 1E 1149.4−6209 IN CRUX: A UNIFIED PICTURE?

G. F. BIGNAMI AND P. A. CARAVEO
Istituto di Fisica Cosmica del C.N.R., Milano

A. GOLDWURM
Dipartimento di Fisica, Università Milano

S. MEREGHETTI[1]
Harvard-Smithsonian Center for Astrophysics

AND

G. G. C. PALUMBO
Istituto TESRE del C.N.R., Bologna
Received 1985 July 1; accepted 1985 September 9

New *EXOSAT* (LE/CMA) and *Einstein Observatory* (IPC and HRI) X-ray data from a region in Crux ($\alpha \approx 11^h45^m$, $\delta \approx 62°$) are reported. Morphological as well as rough spectral analysis of a large ($\sim 1°$) diffuse feature is performed. The diffuse emission is identified with a SNR, a conclusion supported by comparison with existing radio and optical data. The earlier data (1981) of Markert *et al.*, who discovered the feature, are also discussed.

Subject headings: nebulae: supernova remnants — X-rays: sources

I. INTRODUCTION

The region of the Galactic plane around $l = 296°$, $b = -1°$ was explored in soft X-rays using the *Einstein Observatory* (Markert *et al.* 1981; Lamb *et al.* 1980) with the original purpose of mapping a *COS B* high-energy gamma-ray source region (see Caraveo 1983; Bignami and Hermsen 1983) and, subsequently, to better understand its complex X-ray emission. The result was that (1) a new X-ray pulsar (1E 1145−6141) was discovered, solving the problem of the apparent "double" periodicity of 4U 1145−62; and (2) a new extended diffuse feature was seen, which, at the time, had no obvious radio or optical counterpart. Markert *et al.* (1981) classify this feature as a new SNR, separate from the well-known radio and optical SNR G296.1−0.7 also visible in the same IPC field. They consider further the possibility that this new SNR (called 1E 1149.4−6209 from its approximate center coordinates) be interacting with G296.1−0.7. Their analysis, however, was hampered by the fact that, in the IPC field used (see their Fig. 2*a*), one of the counter support ribs happened to fall between the two X-ray structures in the sky.

The region had previously been explored in the optical band by Longmore, Clark, and Murdin (1977) and, more recently, by Hutchings, Crampton, and Cowley (1981). Faint filaments are reported from the region of 1E 1149−6209. In the radio band, Caswell *et al.* (1983) give a new deeper Molonglo 408 MHz map, showing for the first time evidence for a radio counterpart for the larger X-ray structure, thus confirming its SNR nature; they also contend that 1E 1149−6209 is not a separate object but, rather, is part of the general "egg-shaped" radio and X-ray emission from G296.1−0.7.

In what follows, we present unpublished *Einstein Observatory* data as well as recently acquired *EXOSAT* images of the field (see also Mereghetti *et al.* 1985).

The combination of the available X-ray evidence favors the radio-based, single-SNR interpretation with surface emission patchiness, rather than the original proposal by Markert *et al.* (1981) of two separate, and possibly interacting, SNRs.

II. THE *EXOSAT* X-RAY DATA

The *EXOSAT* satellite performed this X-ray observation (pointed at R.A. = $11^h48^m14^s.88$, decl. = $-62°14'58''.98$), with the LE telescope and the CMA focal plane instrument (3000 Å Lexan filter) on 1984 February 12; Figure 1 shows the central part of the raw CMA field. The X-ray data show a complex region, including point sources (none of which was visible in the IPC data of Markert *et al.* 1981) and diffuse emission.

Apart from the known X-ray pulsar 2S 1145−619 (Lamb *et al.* 1980; Warwick, Watson, and Willingale 1985), all the sources but one (source 5) visible in Figure 1 are positionally coincident (within the expected CMA positional accuracy) with bright stars listed in the SAO catalog. Table 1 gives a list of the proposed identifications. Moreover, the photons from sources 1, 4, and 6 were tested for "sum" signal distribution (see, e.g., Caraveo and Bignami 1984), and in all cases such distribution was seen to significantly differ from that obtained both from background regions and from regions of extended (obviously X-ray) emission. As shown in Figure 2, the counts are peaked in the first channels. It is thus legitimate to conclude that the sources are stars. What was seen is their UV component. This rules out the possibility of associating source 6 with an extension of the northern arc, owing to its position and its nonpointlike appearance in the CMA image. In Figure 3 the *EXOSAT* field is presented after a threefold smoothing with a standard Gaussian algorithm with a FWHM of $\sim 100''$. Point sources 3, 4, and 5 of Table 1 and the "hot spot" have been subtracted from the picture. The Molonglo 408 MHz data are also shown for comparison.

III. THE *Einstein Observatory* X-RAY DATA

Table 2 gives a journal of the *Einstein Observatory* IPC and HRI observations of the region. The good coverage was

[1] ESA Fellow.

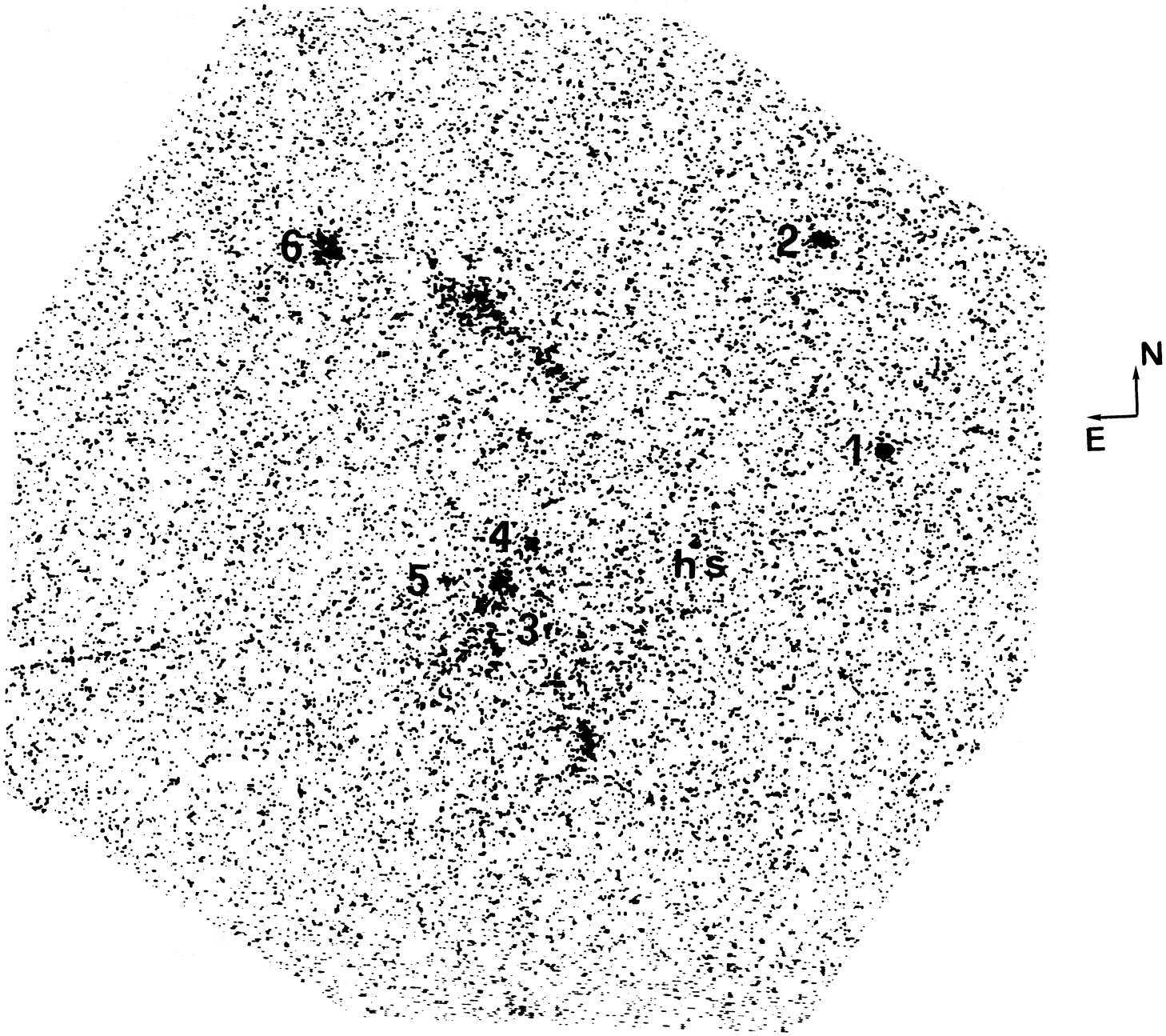

FIG. 1.—Central part (1° × 1°) of the field of the *EXOSAT* Low Energy telescope (CMA detector), centered at R.A. = $11^h48^m15^s88$ decl. = −62°14′58″.98. The extended arc of diffuse emission is seen, together with a number of point sources (numbered 1–6). Source 2 is the X-ray pulsar 2S 1145−619; for the others, see Table 1. "hs" is an instrumental "hot spot."

TABLE 1

PROPOSED IDENTIFICATIONS

Source Number	R.A. (1950)	Decl. (1950)	Identification	m_v	OFFSET (arcsec)
1	$11^h44^m52^s0$	−62° 9′26″.0	SAO 251590	8.6 B2	3.6
2	11 45 32.3	−61 55 55.4	X-ray Pulsar	2S 1145−619	
3	11 47 59.5	−62 22 8.5	SAO 251605	5.6 A2P	8.0
4	11 48 9.9	−62 16 34.7	SAO 251607	8.6 B8	18.1
5	11 48 56.6	−62 19 11.2			
6	11 50 8.8	−61 57 40.3	SAO 251623	7.4 B8	18.2

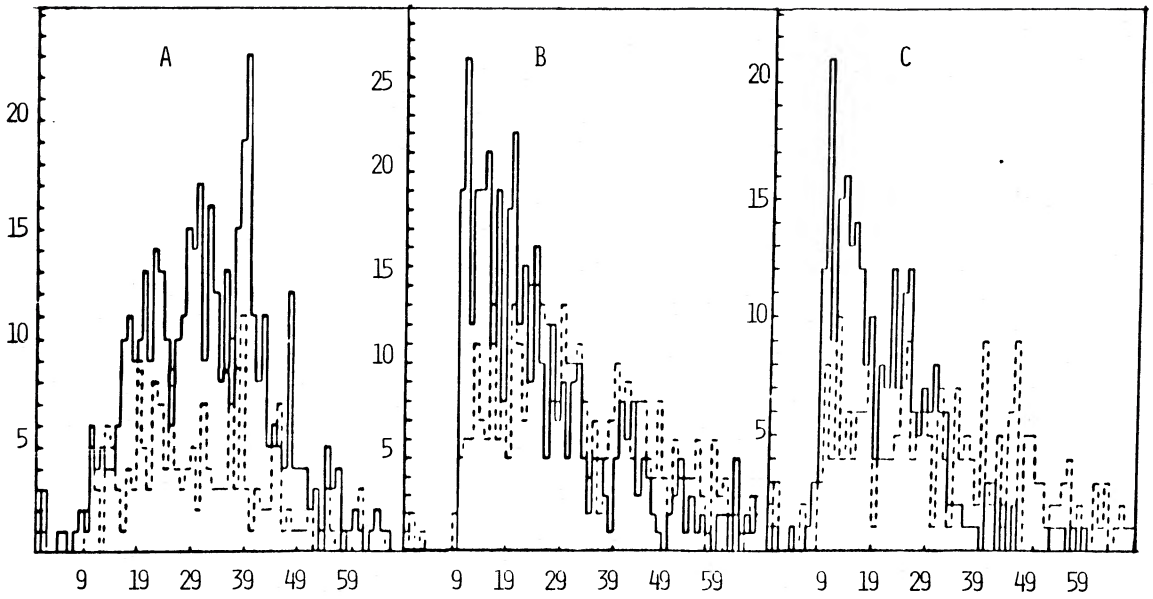

FIG. 2.—Amplitude distribution of CMA "sum" signal, permitting descrimination between UV-dominated emission from a source (lower channels) and true X-ray photons (middle channels). Distribution A is from the bright part of the diffuse emission; B and C are sources 1 and 6 (Table 1), which are positionally coincident with bright stars. Broken lines represent background regions with comparable numbers of counts.

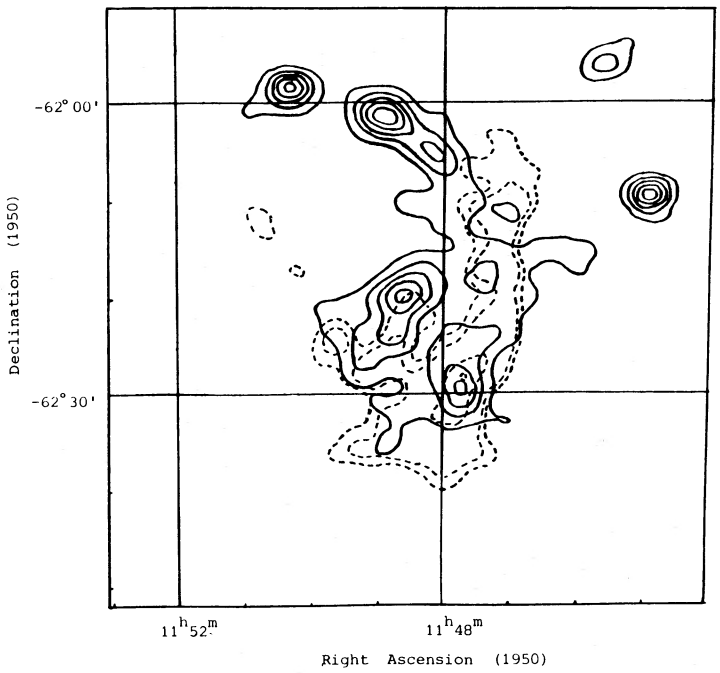

FIG. 3.—Central part of the *EXOSAT* CMA field containing the SNR region. X-ray isophotes are presented after smoothing with a Gaussian algorithm (*full line*) of FWHM ~100″. A sketch of the Molonglo 408 MHz data Caswell and Barnes (1983) is superposed (*broken line*).

TABLE 2

JOURNAL OF OBSERVATIONS

SEQUENCE NUMBER	POINTING DIRECTION R.A.	POINTING DIRECTION Decl.	DATE	ELAPSED TIME (s)	USEFUL TIME (s)
IPC 3942	$11^h49^m14^s9$	−61°47′11″3	1979 Jul 13	1884	1638
IPC 7718	11 50 0.0	−62 11 59.2	1980 Aug 24	11715	5284
IPC 10200	11 48 0.0	−62 29 59.5	1981 Jan 26	4014	2194
HRI 7717	11 48 54.0	−61 59 59.5	1980 Aug 23	26000	19348

obtained in order to study the nearby "twin pulsars" (Lamb *et al.* 1980; White *et al.* 1980).

Figure 4 (Plate 18) shows the HRI field, centered on the northern arc of the diffuse feature. Source 6 in the *EXOSAT* field is not visible, thus confirming its nonassociation with the diffuse northern arc. The image of the arc feature, when studied at full resolution, shows some nonuniform and patchy structure, as expected from a SNR expanding in a dense IS medium.

No point sources are seen in the HRI field.

The IPC data include three fields (I3942, I7718, and I10200). The first two led Markert *et al.* to the discovery of the whole feature (see their Fig. 2*a*), but the pointing direction of I7718 was truly unlucky. One IPC window support "rib" shadowed the central portion of the remnant. Figure 5 (Plate 19) shows the subsequent (1981 January) displaced exposure (I10200) where it is apparent that, although the counter rib did fall in a minimum of X-ray emission, it seems possible to join the emission of the southeast patch with the one of the northern arc. This is further supported by an isophote map of the whole region, shown in Figure 6, obtained by adding the three IPC observations. To produce this mosaic, the photons of energy between 0.2 and 1.7 keV have been summed into array elements of 32″ × 32″. The background has been subtracted and a correction has been applied to take into account the varying exposure across the image (decreasing effective area away from the center of the fields, rib shadows, different useful times of the observations, etc.). Finally, the resulting array has been smoothed with a Gaussian of $\sigma \sim 60''$. The use of spectral information from the IPC, intrinsically limited, is, in this case, further complicated by the presence of heavy IS absorption ($N_H \gtrsim 10^{21}$ cm); Markert *et al.* have already shown that the data appear at least compatible with thermal emission with $0.1 < kT < 0.6$ keV. While it seems difficult to do more in the direction of an absolute spectral shape determination, we have tried to evaluate the constancy of the spectrum across the feature. This was done in two ways: first, IPC pulse-height histograms were constructed for three image regions selected over the SNR, i.e., the northern arc and the south and

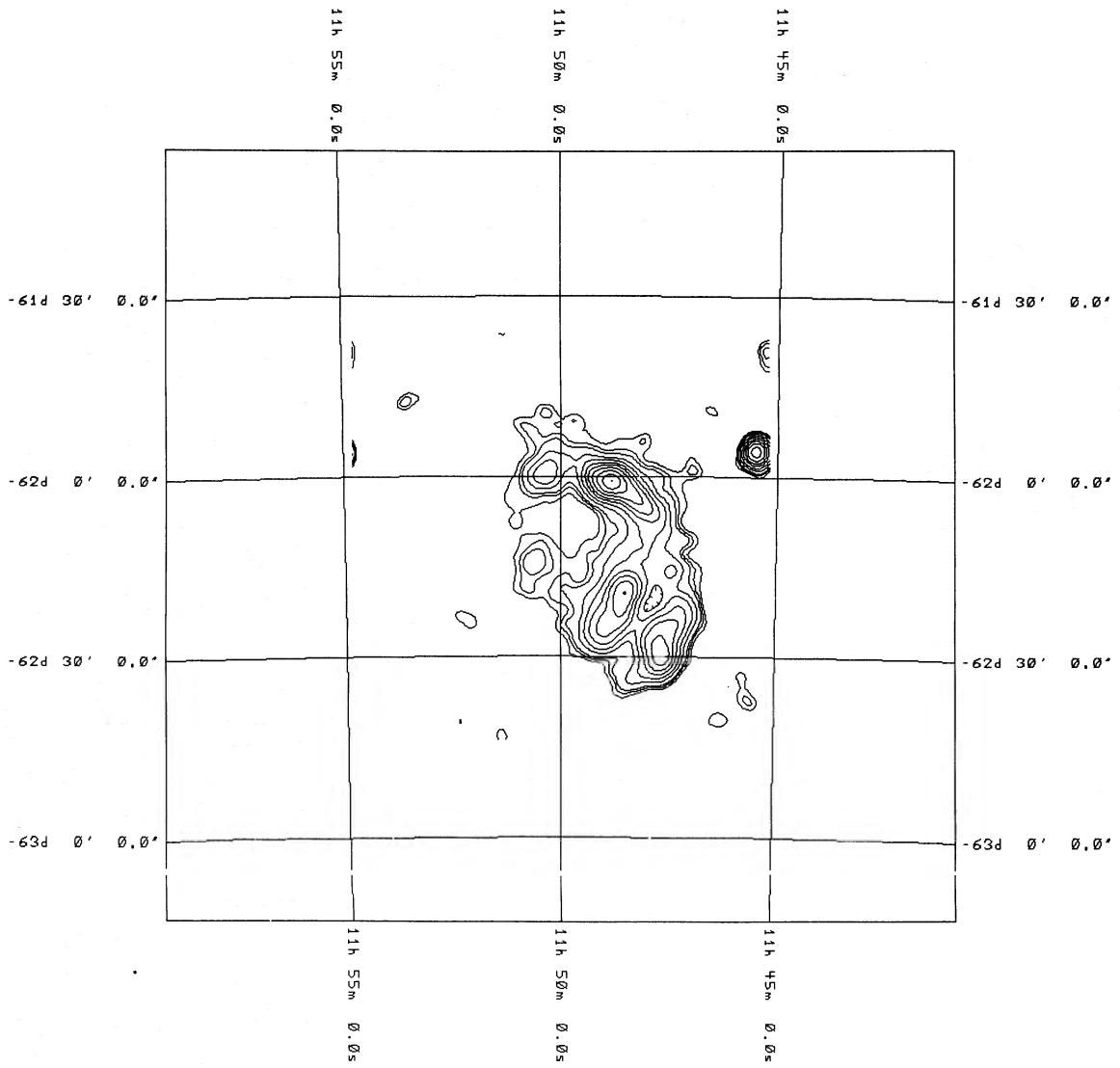

FIG. 6.—Complete *Einstein* X-ray isophote map of the SNR region. Map uses all available IPC data and includes smoothing and corrections for exposure times, vignetting, rib shadows, etc. (see text).

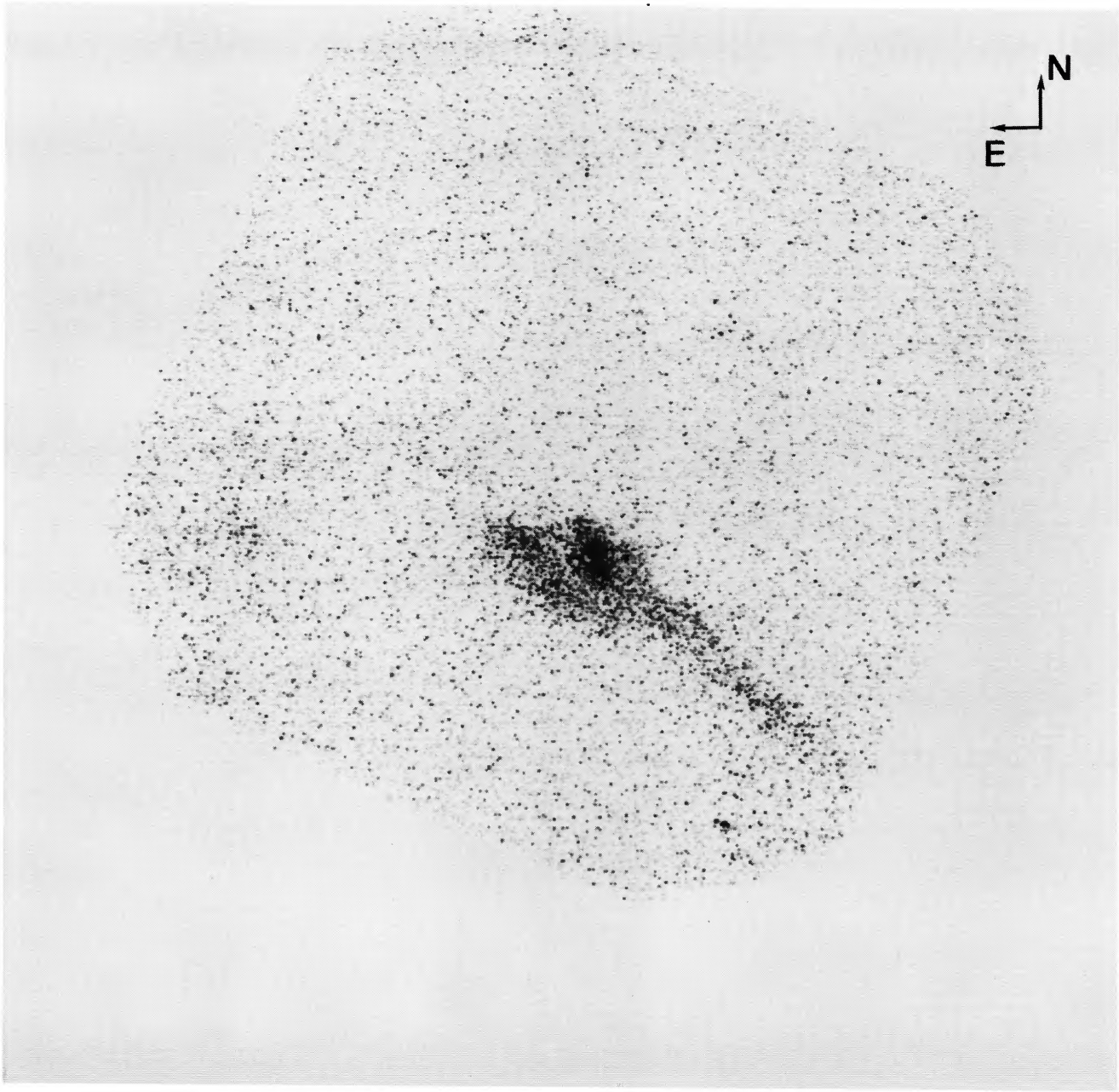

FIG. 4.—*Einstein* HRI field (7717), centered at R.A. = 11^h50^m and decl. = $-61°50'$, so as to cover the "northern arc" of the diffuse feature. Structure within the arc and around it is visible. No point source is found; the clump in the lower right corner also appears filamentary when seen at full resolution.

BIGNAMI *et al.* (see page 609)

PLATE 19

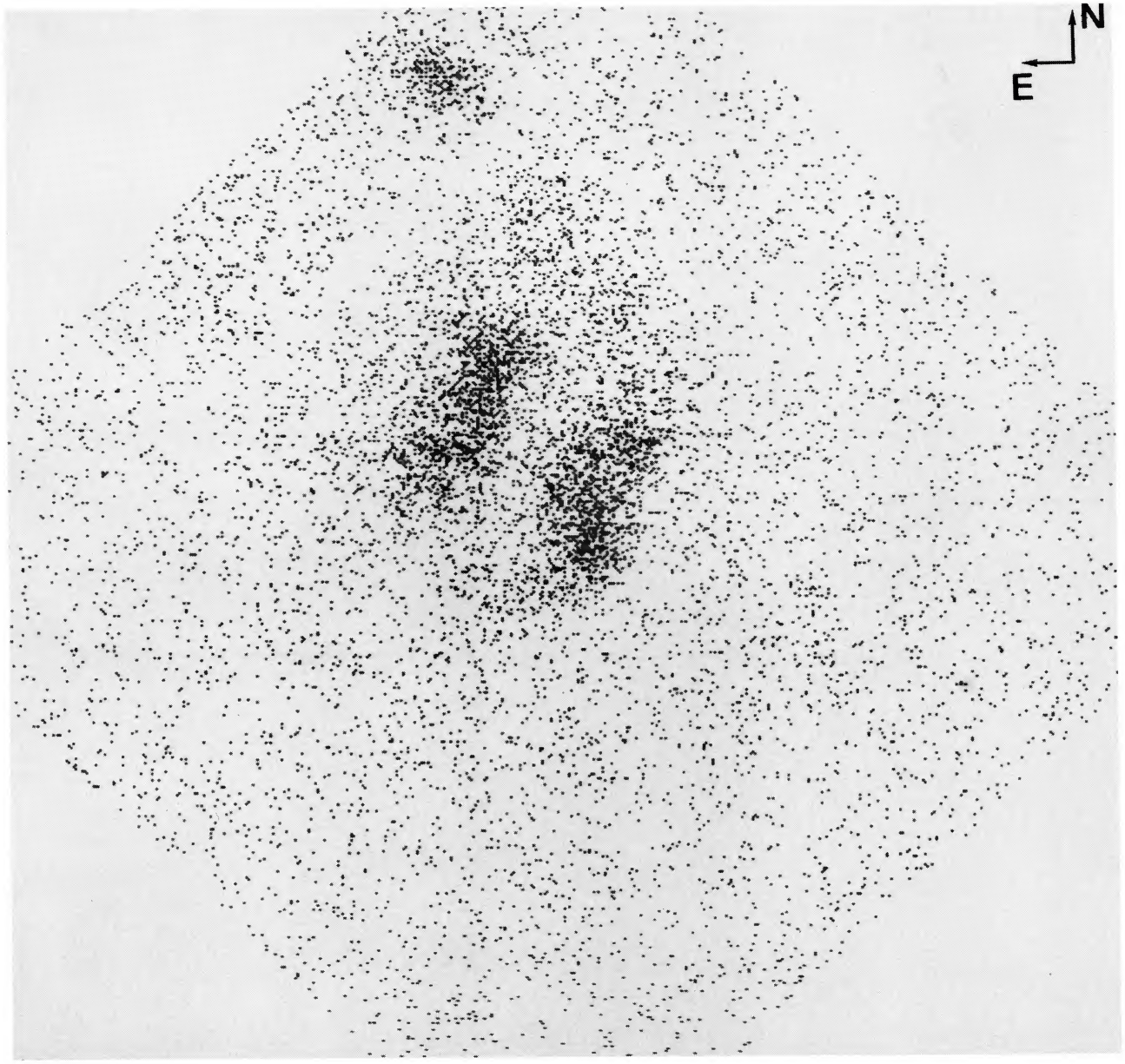

FIG. 5.—*Einstein* IPC field (10200), centered at R.A. = 11^h48^m and decl. = $-62°30'$, i.e., around the two southern "patches." The rib shadowing present in the earlier, northern IPC fields of Markert *et al.* (1981) is now removed.

BIGNAMI *et al.* (see page 609)

southeast patches. No differences in spectral shape were seen across the feature, all distributions being compatible with a soft spectrum with heavy IS absorption. Second, employing a possibly more sensitive method, the "hardness ratio" distribution was constructed as follows. A "soft" (0.16–0.7 keV) and a "hard" (0.7–1.5 keV only, in view of the steep spectrum) IPC band were defined and, after carefully applying the in-flight calibration correction for countergain changes, the ratio H/S was plotted over the image in elements of 32 × 32 pixels (256″ × 256″). No variation can be assigned to the H/S ratio across the whole feature, on this or any other angular scale, going from the northern arc to the southeast "patch."

IV. COMPARISON WITH RADIO AND OPTICAL DATA AND CONCLUSIONS

As in the case of the *EXOSAT* data (Fig. 3), the complete *Einstein* data of Figure 6 can be compared with the 408 MHz radio map of Caswell and Barnes (1983) (Fig. 7 [Pl. 20]). The general agreement now appears quite good, at least as far as the outer dimensions of the object are concerned. The detailed emission regions still do not seem to agree precisely, as it is seen in many radio and X-ray SNRs observed by *Einstein*. This is certainly not a serious problem, however, since this sky region is affected by high obscuration due to a long line of sight through a dense and patchy IS medium. In the X-ray picture of Figure 6 the brightest emission region appears in the northern part, i.e., nearer to the Galactic plane, as expected if the SNR is at 7.7 kpc, with a diameter of ~70 pc and −67 pc away from the Galactic plane. However, Caswell and Barnes (1983) found a contrary situation at 408 MHz and reported such radio behavior as unusual.

Optical studies of the region include those of van den Bergh, Marscher, and Terzian (1973) and Longmore, Clark, and Murdin (1977), who identified the optical nebulosities in the region as a SNR on the basis of several convincing arguments, and the more recent observations by Hutchings, Crampton and Cowley (1981). The latter authors noted the presence of faint Hα and S II nebulosities and arcs which were in qualitative agreement with the X-ray data of Markert *et al.* but which extended well beyond the radio map as it was then known. In the presence of much improved radio and X-ray coverage, the available optical data presently appear somewhat limited, and a deeper study of the region could yield interesting correlative data.

In conclusion, the new X-ray data presented above can be reconciled with the 408 MHz radio picture of one SNR, albeit with large nonuniformities and patchiness in the X-ray emission. This is supported by the lack of evidence for X-ray spectral variations across the feature which also points to a comparable distance for the various parts of the X-ray emission.

However, this last point is quite weak owing to the intrinsic spectral limitations of the IPC. The overall morphology argument also does not hold true for a detailed comparison of the X-ray/radio maps. This is particularly true for the northern arc of the remnant, where to a bright X-ray emission corresponds only a quiet weak radio emission. Better data, especially in the optical, would therefore seem to be needed to confirm the "single" nature of this "crucial" SNR.

It is a pleasure to acknowledge F. Seward for his continuing competent support to the *Einstein* Guest Observers, and Peppo Gavazzi for his skillful help with the artwork. S. M. has been supported at the CfA by an ESA fellowship.

REFERENCES

Bignami, G. F., and Hermsen, W. 1983, *Ann. Rev. Astr. Ap.*, **21**, 67.
Caraveo, P. A. 1983, *Space Sci. Rev.*, **36**, 207.
Caraveo, P. A., and Bignami, G. F. 1984, *Il Nuovo Cimento*, **7C**, 748.
Caswell, J. L., and Barnes, P. J. 1983, *Ap. J. (Letters)*, **271**, L55.
Hutchings, J. B., Crampton, D., and Cowley, A. P. 1981, *A.J.*, **86**, 871.
Lamb, R. C., Markert, T. H., Hartman, R. C., Thompson, D. J., and Bignami, G. F. 1980, *Ap. J.*, **236**, 651.
Longmore, A. J., Clark, D. H., and Murdin, P. 1977, *M.N.R.A.S.*, **181**, 541.
Markert, T. H., Lamb, R. J., Hartman, R. C., Thompson, D. J., and Bignami, G. F. 1981, *Ap. J. (Letters)*, **248**, L17.
Mereghetti, S., Bignami, G. F., Caraveo, P. A., Goldwurm, A., and Palumbo, G. G. C. 1985, *Space Sci. Rev.*, **40**, 495.
van den Bergh, S., Marscher, A. P., and Terzian, Y. 1973, *Ap. J. Suppl.*, **26**, 19.
Warwick, R. S., Watson, M. G., and Willingale, R. 1985, *Space Sci. Rev.*, **40**, 429.
White, N. E., Pravdo, S. H., Becker, R. H., Boldt, E. A., Holt, S. S., and Serlemintsos, P. J. 1980, *Ap. J.*, **239**, 655.

G. F. BIGNAMI and P. A. CARAVEO: Istituto di Fisica Cosmica del C.N.R., Via Bassini, 15, 20133 Milano, Italy

A. GOLDWURM: Dipartimento di Fisica, Università degli Studi, Via Celoria, 16, 20133 Milano, Italy

S. MEREGHETTI: Center for Astrophysics, 60 Garden Street, Cambridge, MA 02138

G. G. C. PALUMBO: I. TESRE del C.N.R., Via De'Castagnoli, 1, 40126 Bologna, Italy

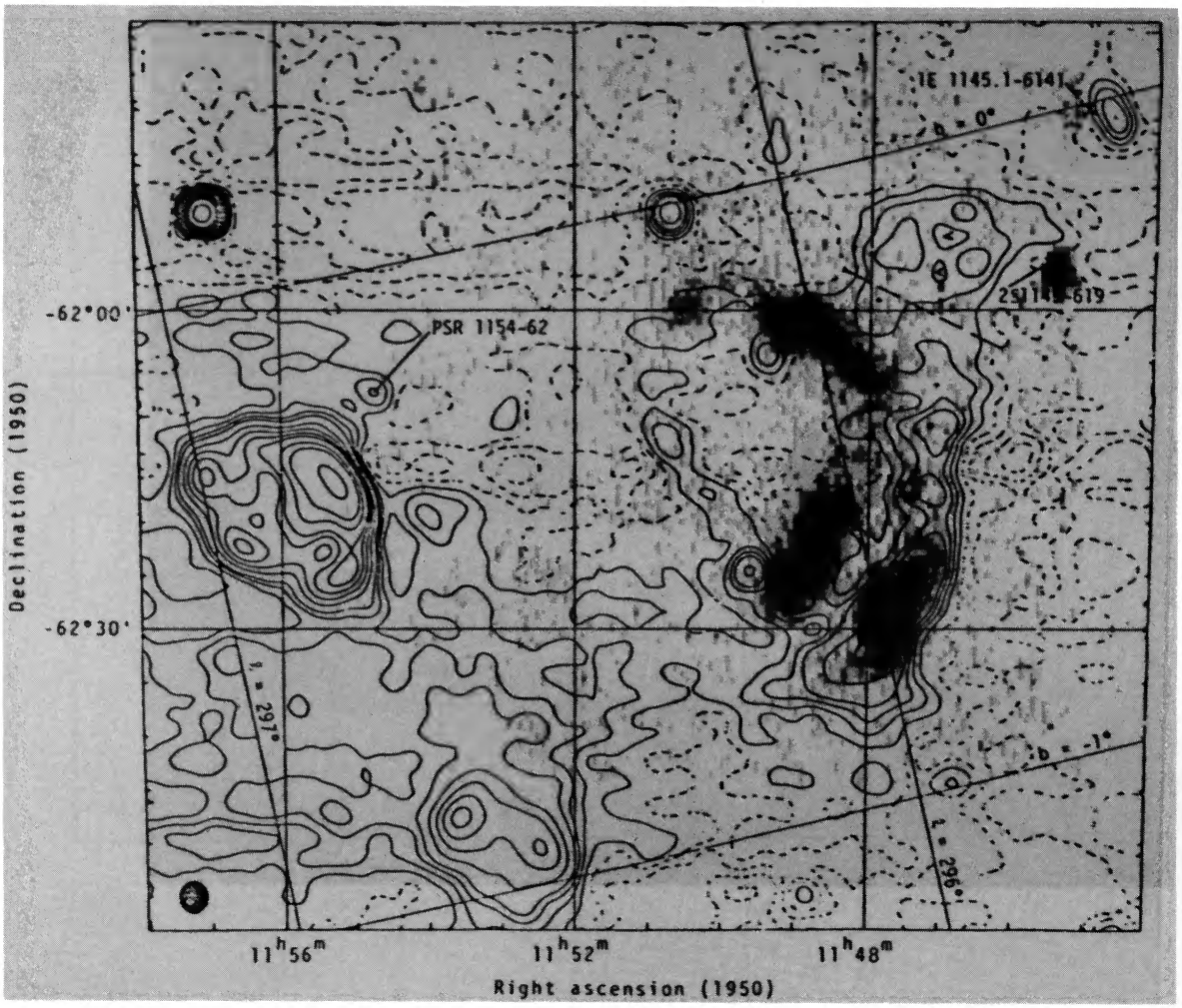

FIG. 7.—Comparison between the *Einstein* X-ray data and the Molonglo 408 MHz map. Radio isophotes are from Fig. 1 of Caswell and Barnes (1983). Gray scale X-ray data are similar to those used for Fig. 6 isophotes.

BIGNAMI *et al.* (see page 610)